Hierarchical Frequency-dependent Chance Constrained Unit Commitment for Bulk AC/DC Hybrid Power Systems with Wind Power Generation

Rui Chen, Deping Ke, Yuanzhang Sun, *Senior Member*, *IEEE*, C. Y. Chung, *Fellow*, *IEEE*, Haotian Wu, Siyang Liao, Jian Xu, *Senior Member*, *IEEE*, and Congying Wei

***Abstract*—As the steady-state frequency of an actual power system decreases from its nominal value, the composite load of the system generally responds positively to lower power consumption, and vice versa. It is believed that this load frequency damping (LFD) effect will be artificially enhanced, i.e., sensitivities of loads with respect to operational frequency will increase, in future power systems. Thus, for wind-integrated power systems, this paper proposes a frequency-dependent chance constrained unit commitment (FDCCUC) model that employs the operational frequency as a dispatching variable so that the LFD effect-based load power can act as a supplemental reserve. Because the frequency deviation is safely restricted, this low-cost reserve can be sufficiently exerted to upgrade the wind power accommodation capability of a power system that is normally confined by an inadequate reserve to cope with uncertain wind power forecasting error. Moreover, when the FDCCUC model is applied to a bulk AC/DC hybrid power system consisting of several independently operated regional AC grids interconnected by DC tie-lines, a hierarchically implemented searching algorithm is proposed to protect private scheduling information of the regional AC grids. Simulations on a 2-area 6-bus system and a 3-area 354-bus system verify the effectiveness of the FDCCUC model and hierarchical searching algorithm.**

***Index Terms*—Unit commitment, AC/DC hybrid power system, load frequency damping, reserve, wind power.**

I. Introduction

Environmental and economic concerns have caused rapid growth in wind power generation (WPG) in recent decades all over the world. However, issues of wind curtailment (WC) and even load shedding (LS) could be serious if there are not adequate reserves prepared in advance to cover the wind power forecasting error [1]. For example, due to lack of operational flexibilities, power systems in China that have relatively tight conventional reserve resources abandoned more than 15% of wind energy generated in 2020 [2].

Although various energy storage systems together with fast-acting gas turbines are high-quality reserve resources for balancing the wind power forecasting error, they generally suffer from immature technique, high expenditure, and insufficient net capacity [3]. Therefore, exploration of technically feasible, low-cost, and abundant reserve resources makes apparent sense for power systems accommodating more wind energy. In recent years, the load frequency damping (LFD) effect has attracted considerable research interest because the active power consumed by the composite load of a power system naturally decreases as the steady-state frequency of the system increases, and vice versa. Because normal power systems can safely operate with frequency deviations within permitted ranges [4], several studies propose flexible frequency operation for multi-microgrids. References [3], [5]-[7] argue that the AC power system operating at a small frequency deviation from the nominal value is compliant and feasible. Based on these research works, AC power systems have great potential to operate flexibly at different frequencies. Therefore, loads become frequency-dependent adjustable resources that participate in power balance control.

It is pointed out in [8] that the natural sensitivity (normally known as the load damping factor) of composite load power with respect to frequency is generally around 1.0-1.5 p.u.. Considerable experience has been gained by industries with respect to technologically upgrading the frequency response capabilities of energy-intensive frequency-dependent industrial loads such as the electrical arc furnace and the polysilicon load. In addition, electrolytic aluminum, another type of industrial energy-intensive load that is connected

Manuscript received: March 10, 2022; revised: June 15, 2022; accepted: August 8, 2022. Date of CrossCheck: August 8, 2022. Date of online publication: September 6, 2022.

This work was supported by the National Natural Science Foundation of China (No. 51777143).

R. Chen, D. Ke (corresponding author), Y. Sun, H. Wu, S. Liao, and J. Xu are with the School of Electrical Engineering and Automation, Wuhan University, Wuhan 430072, China (e-mail: rui-chen@whu.edu.cn; kedeping@whu.edu.cn; yzsun@mail.tsinghua.edu.cn; gswcurry30ww@qq.com; liaosiyang@whu.edu.cn; xujian@whu.edu.cn).

C. Y. Chung is with the Department of Electrical and Computer Engineering, University of Saskatchewan, Saskatoon, SK S7N5A9, Canada (e-mail: c.y.chung@usask.ca).

C. Wei is with the Central China Branch of State Grid Corporation of China, Wuhan 430000, China (e-mail: weicongying@whu.edu.cn).

DOI: 10.35833/MPCE.2022.000138

through the electronic device to the power system, has been proven to have ability to participate in system frequency regulation [9], [10]. Moreover, the residential demand side does witness an increasing trend of power electronic devices such as electric vehicles (EVs) [11]. If such load has willingness to participate in frequency regulation by economic incentive or policy requirement, more power could be released during system frequency excursion, which leads to an increasing trend in frequency damping effect. Based on these, the concept of virtual power plant (VPP) is proposed and extensively studied in recent years to coordinate flexible loads together with distributed energy resources participating in system frequency regulation [12]. Therefore, the frequency sensitivities of composite loads could be positively enhanced for power systems in the near future. Hence, considering the huge capacities of large-scale modern power systems, flexible and abundant frequency-dependent load power is predicted to become much more significant for secure and economic operation of wind-integrated power systems [13].

Generally speaking, wind farms are located in remote areas and integrated into local power grids. Owing to the needs of long transmission distances and large transmission capacities, a common engineering practice is to connect these wind-integrated power grids with power grids feeding load centers by high-voltage DC (HVDC) transmission lines [14]. Voltage source converter (VSC) based HVDC systems have further advantages in terms of bi-directional power transfer between interconnected regional AC grids, which also allows more flexible mutual power (reserve) supports between them [15]. Regional AC grids interconnected by DC tie-lines can have different operational frequencies [16], and this is convenient for fully exerting frequency-dependent loads to engage in the scheduling of entire AC/DC hybrid power systems because each regional AC grid may have its own permitted frequency deviation range. Furthermore, a hierarchical scheduling structure is in general preferred for such AC/DC hybrid power systems because the regional AC grids may be independently operated by different system operators. In other words, due to privacy protection, the regional AC grids may not allow all of their information to be used for centralized scheduling [17].

The aim of this paper is to explore novel reserves that come from the LFD effect for day-ahead generation scheduling of a bulk AC/DC hybrid power system with WPG. Specifically, by allowing feasible deviations of operational frequencies for regional AC grids, the frequency-dependent extra power consumed or supplied by loads can act as partial reserves in an improved stochastic unit commitment problem to cope with the uncertain wind power forecasting error. Moreover, to meet risk preference, the proposed frequency-dependent chance constrained unit commitment (FDCCUC) model explicitly takes into account the wind curtailment expectation (WCE), load shedding expectation (LSE), and chance constrained power balance, which are computed based on the probability distribution of wind power forecasting error. Furthermore, the optimization of the FDCCUC model is approximately converted to a mixed-integer linear programming (MILP) problem and, accordingly, a hierarchical searching algorithm is proposed to find an optimal solution without requiring private scheduling information from the regional AC grids. The main contributions of this paper are summarized as follows.

1) This paper advocates the use of frequency-dependent load power as an auxiliary reserve for the day-ahead scheduling of a WPG-integrated power system. An FDCCUC model is elaborately constructed to adequately exert low-cost reserves based on LFD effects and to guarantee feasible deviations of system operational frequency simultaneously. Thus, from the viewpoint of risk operation, supplemental LFD effect based reserves can considerably increase the accommodation capability of a power system with respect to uncertain WPG.

2) A hierarchical searching algorithm is customized for the FDCCUC model of a bulk AC/DC hybrid power system that consists of several regional AC grids interconnected by DC tie-lines. The algorithm splits the searching process of the original large-scale MILP problem into mutually iterative computations of a master problem and several sub-problems with much smaller size. Each regional AC grid corresponds to one sub-problem that can be privately computed based on the information from the grid. Limited information needs to be exchanged between the system-level master problem and the sub-problems, allowing private scheduling information of the independently operated regional AC grids to be hidden and protected during the searching process.

The rest of paper is organized as follows. Section II formulates the FDCCUC model for bulk AC/DC hybrid power systems with WPG. Section III presents the details of the hierarchical searching algorithm for FDCCUC model to protect private scheduling information of regional AC grids. Numerical simulations are conducted in Section IV. Finally, Section V concludes the paper.

II. Formulation of FDCCUC Model for Bulk AC/DC Hybrid Power Systems with WPG

This paper deals with day-ahead scheduling of AC/DC hybrid power systems comprised of multiple large-scale regional AC grids interconnected by DC tie-lines. As shown in Fig. 1, regional AC grids are usually operated by different independent system operators while DC tie-lines are under the regulation of a high-level system-wide operator. These regional AC grids can be synchronously decoupled so that they can work at steady states with distinct frequencies. Given a general AC grid that operates at a nominal frequency, additional power will be released or consumed by the composite load when the steady-state frequency of the grid deviates from the nominal value, which depends on the frequency damping characteristic of the composite load, as follows [8]:

$$\Delta P = -K^{\mathrm{L}} \Delta f \tag{1}$$

where ΔP is the aggregated power adjustment of loads due to the frequency deviation Δf; and K^{L} is the aggregated sensitivity coefficient of load power with respect to Δf. Therefore, taking advantage of the additional power reserve associated with the LFD effect, this paper proposes that all region-

al AC grids can have different and time-varying operational frequencies as long as they remain within permitted safe ranges; random wind power forecasting errors can thus be partially covered by the LFD-based load reserve that, along with conventional reserves, is shared among the regional AC grids through DC tie-lines. Subsequently, a proposed FDC-CUC model is formulated for AC/DC hybrid power systems with WPG.

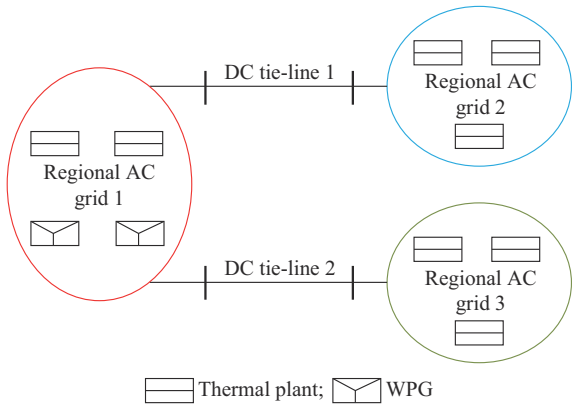

Fig. 1. Bulk AC/DC hybrid power system with WPG.

Remark: it should be noted that the proposed auxiliary reserve from LFD effect could be conflict with existing secondary frequency control, i.e., eliminating frequency deviation. Whereas, the research in this paper is consistent with existing unit commitment research that provides thermal units with a preliminary reference operation strategy based on the forecasting load demand and renewable output in day-ahead time frame. Then the actual generation output is regulated by economical dispatch through secondary frequency control based on actual operational conditions with short-term load and renewable power prediction. Even so, this paper is an exploratory research focusing on potential operational strategy for the future power system with extreme high renewable penetration level. This paper attempts to facilitate the maximum renewable power without the unbridled expansion of traditional reserve services. Besides, introducing the proposed auxiliary reserve from LFD effect in unit commitment schedule could decrease the requirement for expensive fast-response reserve resources [3]. Therefore, the coordination with secondary frequency control is not considered in this paper, which is consistent with the state-of-the-art unit commitment studies.

A. Objective of FDCCUC Model

For the AC/DC hybrid power system studied in this paper, the objective of the FDCCUC model is presented as:

$$\min\ C^{\mathrm{Total}}=\sum_{m\in A}C_m^{\mathrm{Total}}=\sum_{m\in A}\left(C_m^{\mathrm{Th}}+C_m^{\mathrm{Rs}}+C_m^{\mathrm{Risk}}+C_m^{\mathrm{Freq}}\right) \tag{2}$$

$$C_m^{\mathrm{Th}}=\sum_{t\in T}\sum_{i\in G_m}\left(C_{m,i}^{\mathrm{SU}}v_{m,i,t}+C_{m,i}^{\mathrm{SD}}z_{m,i,t}\right)+\sum_{t\in T}\sum_{i\in G_m}\left(a_{m,i}+b_{m,i}P_{m,i,t}^{\mathrm{Th}}+c_{m,i}\left(P_{m,i,t}^{\mathrm{Th}}\right)^2\right) \tag{3}$$

$$C_m^{\mathrm{Rs}}=\sum_{t\in T}\sum_{i\in G_m}\left(RC_{m,i}^{\mathrm{Up}}\cdot R_{m,i,t}^{\mathrm{Up}}+RC_{m,i}^{\mathrm{Dn}}\cdot R_{m,i,t}^{\mathrm{Dn}}\right) \tag{4}$$

$$C_m^{\mathrm{Risk}}=\sum_{t\in T}\left(C_m^{\mathrm{LS}}Q_{m,t}^{\mathrm{LSE}}+C_m^{\mathrm{WC}}Q_{m,t}^{\mathrm{WCE}}\right) \tag{5}$$

$$C_m^{\mathrm{Freq}}=\pi_m\sum_{t\in T}\left(\Delta f_{m,t}^{+}+\Delta f_{m,t}^{-}\right) \tag{6}$$

where C^{Total} is the total operating cost (OC) of the AC/DC hybrid power system; C_m^{Total} is the total OC of the m^{th} regional AC grid; C_m^{Th} is the OC of all thermal units located at the m^{th} regional AC grid; C_m^{Rs} is the reserve cost (RC) of the m^{th} regional AC grid; C_m^{Risk} is the cost relevant to operational risk preference of the m^{th} regional AC grid; C_m^{Freq} is the penalty cost of frequency deviation; $v_{m,i,t}$ and $z_{m,i,t}$ are the binary variables (0/1) that indicate startup ($v=1$) and shutdown ($z=1$) manipulations of the i^{th} thermal unit at the m^{th} regional AC grid at time t, respectively; $C_{m,i}^{\mathrm{SU}}$ and $C_{m,i}^{\mathrm{SD}}$ are the startup and shutdown cost coefficients, respectively; $P_{m,i,t}^{\mathrm{Th}}$ is the scheduled power output of the i^{th} thermal unit at the m^{th} regional AC grid at time t; $a_{m,i}$, $b_{m,i}$, and $c_{m,i}$ are the fuel cost coefficients of the i^{th} thermal unit at the m^{th} regional AC grid; $R_{m,i,t}^{\mathrm{Up}}$ and $R_{m,i,t}^{\mathrm{Dn}}$ are the upward and downward reserves generated by the i^{th} thermal unit at the m^{th} regional AC grid at time t, respectively; $RC_{m,i}^{\mathrm{Up}}$ and $RC_{m,i}^{\mathrm{Dn}}$ are the cost coefficients of upward and downward reserves of the i^{th} thermal unit at the m^{th} regional AC grid, respectively; $Q_{m,t}^{\mathrm{WCE}}$ and $Q_{m,t}^{\mathrm{LSE}}$ are the WCE and LSE of the m^{th} regional AC grid at time t, respectively; C_m^{WC} and C_m^{LS} are the cost coefficients of the m^{th} regional AC grid; $\Delta f_{m,t}^{+}$ and $\Delta f_{m,t}^{-}$ are the auxiliary variables for positive and negative frequency deviation, respectively; π_m is the penalty coefficient of the frequency deviation, and the determination and sensitivity analysis of π_m is discussed in Section IV-B; A is the set of indexes of all regional AC grids; T is the set of all dispatching time instants over the scheduling horizon; and G_m is the set of indexes of all thermal units located at the m^{th} regional AC grid.

The risk cost induced by overestimating and underestimating the WPG is specifically considered in this paper, as shown in (5). As mentioned previously, LFD effect based power reserves can simply be harnessed by shifting operational frequencies of regional AC grids from their nominal values. However, the frequency deviations must be minimized. So, $\Delta f_{m,t}^{+}$ and $\Delta f_{m,t}^{-}$ in (6) are utilized with two considerations: to express the frequency deviation (the detailed expression will be introduced later) and to enable the use of linear equation (6) in the objective function equivalent to penalization of the absolute value of the frequency deviation.

B. Constraints of FDCCUC Model

1) Constraints on DC Tie-lines Among Regional AC Grids

In this paper, DC tie-lines of the AC/DC hybrid power system are treated as generating sources with respect to all regional AC grids, indicating that power as well as reserves of the DC tie-lines are actually injected to the AC grids if signs of these variables are positive, and vice versa. Thus, the following relationships should be naturally hold:

$$\sum_{m\in A,r\in R}P_{m,r,t}^{\mathrm{TLine}}=0 \tag{7}$$

$$\sum_{m\in A,r\in R}TR_{m,r,t}^{\mathrm{Up}}=0 \tag{8}$$

$$\sum_{m\in A, r\in R} TR^{\mathrm{Dn}}_{m,r,t}=0 \tag{9}$$

$$-\sum_{r\in R} TR^{\mathrm{Up}}_{m,r,t}\le \sum_{i\in G_m} R^{\mathrm{Up}}_{m,i,t} \tag{10}$$

$$-\sum_{r\in R} TR^{\mathrm{Dn}}_{m,r,t}\le \sum_{i\in G_m} R^{\mathrm{Dn}}_{m,i,t} \tag{11}$$

where $P^{\mathrm{Tline}}_{m,r,t}$ is the scheduled power received by the m^{th} regional AC grid from the r^{th} DC tie-line at time t; $TR^{\mathrm{Up}}_{m,r,t}$ and $TR^{\mathrm{Dn}}_{m,r,t}$ are the scheduled upward and downward reserves provided by the r^{th} DC tie-line for the m^{th} regional AC grid at time t, respectively; and R is the set of indexes of all DC tie-lines.

Constraints (7)-(9) guarantee the power and upward/downward reserve at both ends of one single DC tie-line keep balance at any dispatching interval. Constraints (10) and (11) mean that, in practice, the reserve power delivered from a regional AC grid by the DC tie-lines should be less than the total reserve of this grid.

To safely operate the DC tie-lines engaged in transmission of scheduled power as well as reserves among regional AC grids, the following technical constraints should be included [15]:

$$-CP^{\mathrm{Tline}}_r\le P^{\mathrm{Tline}}_{m,r,t}+TR^{\mathrm{Up}}_{m,r,t}\le CP^{\mathrm{Tline}}_r \tag{12}$$

$$-CP^{\mathrm{Tline}}_r\le P^{\mathrm{Tline}}_{m,r,t}-TR^{\mathrm{Dn}}_{m,r,t}\le CP^{\mathrm{Tline}}_r \tag{13}$$

$$-CP^{\mathrm{Tline}}_r\le P^{\mathrm{Tline}}_{m,r,t+1}+TR^{\mathrm{Up}}_{m,r,t+1}-P^{\mathrm{Tline}}_{m,r,t}-TR^{\mathrm{Up}}_{m,r,t}\le CP^{\mathrm{Tline}}_r \tag{14}$$

$$-CP^{\mathrm{Tline}}_r\le P^{\mathrm{Tline}}_{m,r,t+1}+TR^{\mathrm{Up}}_{m,r,t+1}-P^{\mathrm{Tline}}_{m,r,t}+TR^{\mathrm{Dn}}_{m,r,t}\le CP^{\mathrm{Tline}}_r \tag{15}$$

$$-CP^{\mathrm{Tline}}_r\le P^{\mathrm{Tline}}_{m,r,t+1}-TR^{\mathrm{Dn}}_{m,r,t+1}-P^{\mathrm{Tline}}_{m,r,t}+TR^{\mathrm{Dn}}_{m,r,t}\le CP^{\mathrm{Tline}}_r \tag{16}$$

$$-CP^{\mathrm{Tline}}_r\le P^{\mathrm{Tline}}_{m,r,t+1}-TR^{\mathrm{Up}}_{m,r,t+1}-P^{\mathrm{Tline}}_{m,r,t}-TR^{\mathrm{Up}}_{m,r,t}\le CP^{\mathrm{Tline}}_r \tag{17}$$

where CP^{Tline}_r is the permitted maximum power change of the DC tie-line. Constraints (12)-(17) commonly ensure that the actual power of the DC tie-line cannot be overloaded and very abruptly changed, taking into account the reserves.

2) Constraints on Power Balance and Chance Constraints Against Wind Power Uncertainties Within Regional AC Grids

The power balance must be held within all regional AC grids by the following constraints:

$$\sum_{i\in G_m} P^{\mathrm{Th}}_{m,i,t}+\sum_{r\in R} P^{\mathrm{Tline}}_{m,r,t}+WPF_{m,t}+\Delta P^{\mathrm{Freq}}_{m,t}-P^{\mathrm{Load}}_{m,t}=0 \tag{18}$$

$$\Delta P^{\mathrm{Freq}}_{m,t}=-K^{\mathrm{L}}_{m,t}\Delta f_{m,t} \tag{19}$$

$$\Delta f_{m,t}=\Delta f^{+}_{m,t}-\Delta f^{-}_{m,t} \tag{20}$$

$$\begin{cases} 0\le \Delta f^{+}_{m,t}\le \Delta f^{\max}_{m} \\ 0\le \Delta f^{-}_{m,t}\le \Delta f^{\max}_{m} \end{cases} \tag{21}$$

where $WPF_{m,t}$ is a deterministic value that represents the aggregated wind power forecasting of the m^{th} regional AC grid at future time t; $\Delta f_{m,t}$ is the frequency deviation from the nominal value of the m^{th} regional AC grid at future time t; $\Delta f^{\max}_{m}$ is the permitted maximum frequency deviation in the steady state of the m^{th} regional AC grid; $P^{\mathrm{Load}}_{m,t}$ is the aggregation of all nominal loads of the m^{th} regional AC grid at future time t; $\Delta P^{\mathrm{Freq}}_{m,t}$ is the extra power supplied or consumed by the loads due to LFD effects of the m^{th} regional AC grid at future time t; and $K^{\mathrm{L}}_{m,t}$ is the aggregated power sensitivity of the loads with respect to the frequency deviation of the m^{th} regional AC grid at future time t.

It can be observed from (7) and (18) that the power capacities contributed by the LFD effects are shared among all regional AC grids through the DC tie-lines. Furthermore, via the connections with thermal units in (16), the LFD-based power capacities can spare the capacities of some thermal units, which are then used as reserves. Therefore, the operational reliability of each regional AC grid against the uncertainties of wind power (forecasting error) is guaranteed by the following chance constraints:

$$\Pr\left\{\sum_{i\in G_m} R^{\mathrm{Up}}_{m,i,t}+\sum_{r\in R} TR^{\mathrm{Up}}_{m,r,t}\ge WPFE_{m,t}\right\}\ge \bar{c}_m \tag{22}$$

$$\Pr\left\{-\left(\sum_{i\in G_m} R^{\mathrm{Dn}}_{m,i,t}+\sum_{r\in R} TR^{\mathrm{Dn}}_{m,r,t}\right)\le WPFE_{m,t}\right\}\ge \underline{c}_m \tag{23}$$

where $WPFE_{m,t}$ is a random variable that represents the aggregated wind power forecasting error of the m^{th} regional AC grid at future time t; $\Pr\{\cdot\}$ denotes the operator that derives occurrence probability of the event inside the curly braces; and $\bar{c}_m$ and $\underline{c}_m$ are the confidence levels of the m^{th} regional AC grid.

Chance constraints (22) and (23) can be straightforwardly interpreted as a given confidence to cover the uncertain overestimation ($WPFE_{m,t}>0$) or underestimation ($WPFE_{m,t}<0$) of wind power by the regional and cross-regional reserves. In other words, the probabilities of LS and WC events due to wind power forecasting error can be adequately restricted.

3) Constraints on Thermal Units Within Regional AC Grids

As usual, common technical constraints are imposed on thermal units as:

$$v_{m,i,t}+z_{m,i,t}\le 1 \tag{24}$$

$$u_{m,i,t}-u_{m,i,t-1}=v_{m,i,t}-z_{m,i,t} \tag{25}$$

$$v_{m,i,t}T^{\mathrm{on}}_{\min}\le \sum_{\tau=0}^{T^{\mathrm{on}}_{\min}-1} u_{m,i,t+\tau} \tag{26}$$

$$z_{m,i,t}T^{\mathrm{off}}_{\min}\le \sum_{\tau=0}^{T^{\mathrm{on}}_{\min}-1}\left(1-u_{m,i,t+\tau}\right) \tag{27}$$

$$u_{m,i,t}P^{\mathrm{Th,min}}_{m,i}\le P^{\mathrm{Th}}_{m,i,t}\le u_{m,i,t}P^{\mathrm{Th,max}}_{m,i} \tag{28}$$

$$P^{\mathrm{Th}}_{m,i,t}-P^{\mathrm{Th}}_{m,i,t-1}\le \left(1-v_{m,i,t}\right)\cdot RR^{\mathrm{Up}}_{m,i}-R^{\mathrm{Up}}_{m,i,t}+v_{m,i,t}P^{\mathrm{Th,max}}_{m,i} \tag{29}$$

$$P^{\mathrm{Th}}_{m,i,t}-P^{\mathrm{Th}}_{m,i,t-1}\ge \left(z_{m,i,t}-1\right)\cdot RR^{\mathrm{Dn}}_{m,i}+R^{\mathrm{Dn}}_{m,i,t}-z_{m,i,t}P^{\mathrm{Th,max}}_{m,i} \tag{30}$$

$$0\le R^{\mathrm{Up}}_{m,i,t}\le \min\left\{P^{\mathrm{Th,max}}_{m,i}u_{m,i,t}-P^{\mathrm{Th}}_{m,i,t}, RR^{\mathrm{Up}}_{m,i}\right\} \tag{31}$$

$$0\le R^{\mathrm{Dn}}_{m,i,t}\le \min\left\{P^{\mathrm{Th}}_{m,i,t}-P^{\mathrm{Th,min}}_{m,i}u_{m,i,t}, RR^{\mathrm{Dn}}_{m,i}\right\} \tag{32}$$

where $v_{m,i,t}$ and $z_{m,i,t}$ are the binary variables (0/1) indicating the startup ($v_{m,i,t}=1$) and shutdown ($z_{m,i,t}=1$) operations of the i^{th} thermal unit at the m^{th} regional AC grid at time t, respectively; $u_{m,i,t}$ is a binary variable representing the on/off states of the i^{th} thermal unit (1-on, 0-off) at the m^{th} regional AC grid at time t; $T^{\mathrm{on}}_{\min}$ and $T^{\mathrm{off}}_{\min}$ are the required minimum

durations when the state of thermal units are on and off, respectively; $P_{m,i}^{\mathrm{Th,max}}$ and $P_{m,i}^{\mathrm{Th,min}}$ are the allowable maximum and minimum power outputs of the i^{th} thermal unit at the m^{th} regional AC grid, respectively; and $RR_{m,i}^{\mathrm{Up}}$ and $RR_{m,i}^{\mathrm{Dn}}$ are the maximum ramp-up and ramp-down speeds of the i^{th} thermal units at the m^{th} regional AC grid, respectively.

Constraints (24)-(32) are not further explained here, and the related descriptions can refer to [18].

Specifically, constraints (7)-(32) may need to be enumerated as:

$$\forall m \in A, \forall i \in G_m, \forall r \in R, \forall t \in T \tag{33}$$

C. Computations of Q^{LSE}, Q^{WCE}, and Chance Constraints and Linearization

Clearly, detailed computations of Q^{LSE}, Q^{WCE}, and chance constraints (22) and (23) will complete the formation of the scheduling problem (2)-(33). These computations are essentially based on the probability distribution of wind power forecasting error. A general approach to derive the probability density function (PDF) of wind power forecasting error is to fit a large amount of historical error data to a parameterized distribution function, for example, the parameterized Gaussian function [19]. In this paper, the versatile probability distribution is employed to approximate the PDF of $WPFE_{m,t}$ as:

$$f_m\left(WPFE_{m,t}\right) = \frac{\alpha_m \beta_m \mathrm{e}^{-\alpha_m\left(WPFE_{m,t}-\gamma_m\right)}}{\left(1+\mathrm{e}^{-\alpha_m\left(WPFE_{m,t}-\gamma_m\right)}\right)^{\beta_m+1}} \tag{34}$$

where α_m, β_m, and γ_m are the tunable shaping parameters, and the details can be found in [18] with respect to the derivation of these parameters based on the curve fitting of historical error data.

Figure 2 shows the typical curve of a versatile probability distribution. Analogous to the measure employed in [1], it is simply believed that LS and WC occur when the wind power forecasting error exceeds the total upward and downward reserves, respectively. Then, according to Fig. 2, LS and WC expectations can be integrated based on the concept of conditional value-at-risk (CVaR) as [18]:

$$Q_{m,t}^{\mathrm{LSE}} = \int_{\sum_{i\in G_m} R_{m,i,t}^{\mathrm{Up}} + \sum_{r\in R} R_{m,r,t}^{\mathrm{Up}}}^{+\infty} \left(x - \sum_{i\in G_m} R_{m,i,t}^{\mathrm{UP}} - \sum_{i\in R} R_{m,r,t}^{\mathrm{UP}}\right) f_m(x)\,\mathrm{d}x \tag{35}$$

$$Q_{m,t}^{\mathrm{WCE}} = \int_{-\left(\sum_{i\in G_m} R_{m,i,t}^{\mathrm{Dn}} + \sum_{r\in R} R_{m,r,t}^{\mathrm{Dn}}\right)}^{-\infty} \left(x + \sum_{i\in G_m} R_{m,i,t}^{\mathrm{Dn}} + \sum_{i\in R} R_{m,r,t}^{\mathrm{Dn}}\right) f_m(x)\,\mathrm{d}x \tag{36}$$

where $Q_{m,t}^{\mathrm{LSE}}$ and $Q_{m,t}^{\mathrm{WCE}}$ are the monotonic functions of the total upward reserve $\sum R_{m,i,t}^{\mathrm{Up}} + \sum R_{m,r,t}^{\mathrm{Up}}$ and total downward reserve $\sum R_{m,i,t}^{\mathrm{Dn}} + \sum R_{m,r,t}^{\mathrm{Dn}}$, respectively.

Chance constraints (22) and (23) can be calculated based on (34) as:

$$\sum_{i\in G_m} R_{m,i,t}^{\mathrm{Up}} + \sum_{r\in R} TR_{m,r,t}^{\mathrm{Up}} \geq F_m^{-1}\left(\bar{c}_m\right) \tag{37}$$

$$\sum_{i\in G_m} R_{m,i,t}^{\mathrm{Dn}} + \sum_{r\in R} TR_{m,r,t}^{\mathrm{Dn}} \geq -F_m^{-1}\left(1-\underline{c}_m\right) \tag{38}$$

where $F_m^{-1}(\cdot)$ is the inverse function of the cumulative distribution function (CDF) of $WPFE_{m,t}$. Interestingly, $F_m^{-1}(\cdot)$ is also analytical [18].

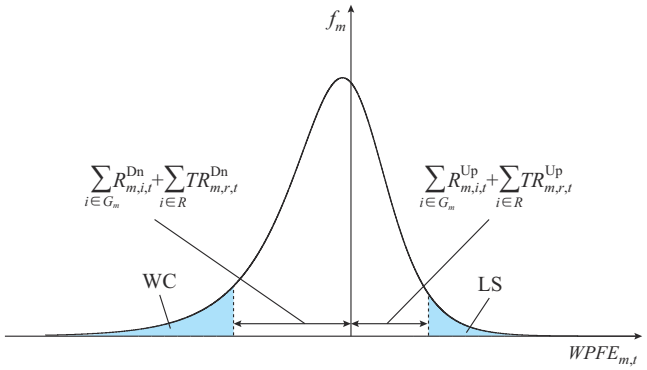

Fig. 2. Illustration of WC and LS according to PDF of a wind farm.

The optimization (2)-(36) is a mixed-integer nonlinear programming (MINLP) problem due to the nonlinearities introduced by (3), (35), and (36). Solving a large-scale and general MINLP problem directly is not easy nor convenient, with MILP problems being more favorable. According to (35), (36), and Fig. 2, $Q_{m,t}^{\mathrm{LSE}}$ and $Q_{m,t}^{\mathrm{WCE}}$ can be piecewise linearized. Thus, Fig. 3 schematically illustrates the curves of these two functions and relevant piecewise linearization. Then, (35) and (36) can be approximately replaced by:

$$Q_{m,t}^{\mathrm{LSE}} = LSE_m^0 + \sum_{\tau=1}^{N_{\mathrm{LS}}} k_{m,\tau}^{\mathrm{LS}} \delta_{m,\tau}^{\mathrm{Up}} \tag{39}$$

$$\sum_{i\in G_m} R_{m,i,t}^{\mathrm{Up}} + \sum_{r\in R} TR_{m,r,t}^{\mathrm{Up}} = \sum_{\tau=1}^{N_{\mathrm{LS}}} \delta_{m,\tau}^{\mathrm{Up}} \tag{40}$$

$$0 \leq \delta_{m,1}^{\mathrm{Up}} \leq S_{m,1}^{\mathrm{Up}} \tag{41}$$

$$0 \leq \delta_{m,\tau}^{\mathrm{Up}} \leq S_{m,\tau}^{\mathrm{Up}} - S_{m,\tau-1}^{\mathrm{Up}} \quad \forall \tau \in \left\{2,3,\ldots,N_{\mathrm{LS}}\right\} \tag{42}$$

$$Q_{m,t}^{\mathrm{WCE}} = WCE_m^0 + \sum_{\tau=1}^{N_{\mathrm{WC}}} k_{m,\tau}^{\mathrm{WC}} \delta_{m,\tau}^{\mathrm{Dn}} \tag{43}$$

$$\sum_{i\in G_m} R_{m,i,t}^{\mathrm{Dn}} + \sum_{r\in R} TR_{m,r,t}^{\mathrm{Dn}} = \sum_{\tau=1}^{N_{\mathrm{WC}}} \delta_{m,\tau}^{\mathrm{Dn}} \tag{44}$$

$$0 \leq \delta_{m,1}^{\mathrm{Dn}} \leq S_{m,1}^{\mathrm{Dn}} \tag{45}$$

$$0 \leq \delta_{m,\tau}^{\mathrm{Dn}} \leq S_{m,\tau}^{\mathrm{Dn}} - S_{m,\tau-1}^{\mathrm{Dn}} \quad \forall \tau \in \left\{2,3,\ldots,N_{\mathrm{WC}}\right\} \tag{46}$$

where LSE_m^0 and WCE_m^0 are the initial values of $Q_{m,t}^{\mathrm{LSE}}$ and $Q_{m,t}^{\mathrm{WCE}}$ when the upward and downward reserves are zero, respectively; N_{LS} and N_{WC} are the numbers of linear line segments employed for approximating $Q_{m,t}^{\mathrm{LSE}}$ and $Q_{m,t}^{\mathrm{WCE}}$, respectively; $S_{m,\tau}^{\mathrm{Up}}$ and $S_{m,\tau}^{\mathrm{Dn}}$ denote the τ^{th} vertices of linear line segments for $Q_{m,t}^{\mathrm{LSE}}$ and $Q_{m,t}^{\mathrm{WCE}}$, respectively; $\delta_{m,\tau}^{\mathrm{Up}}$ and $\delta_{m,\tau}^{\mathrm{Dn}}$ are the τ^{th} increments with respect to these vertices; and $k_{m,\tau}^{\mathrm{LS}}$ and $k_{m,\tau}^{\mathrm{WC}}$ are the τ^{th} slopes of the linear line segments. Analogously, (3) can also be piecewise linearized as:

$$C_m^{\mathrm{Th}}=\sum_{t\in T}\sum_{i\in G_m}\left(C_{m,i}^{\mathrm{SU}}v_{m,i,t}+C_{m,i}^{\mathrm{SD}}z_{m,i,t}\right)+\sum_{i\in G_m}\sum_{\tau=1}^{N_i^{\mathrm{Th}}}\left(FC_{m,i}^{\mathrm{Th},0}+k_{m,i,\tau}^{\mathrm{Th}}\delta_{m,i,\tau}^{\mathrm{Th}}\right) \tag{47}$$

$$P_{m,i,t}^{\mathrm{Th}}=\sum_{\tau=1}^{N_i^{\mathrm{Th}}}\delta_{m,i,\tau}^{\mathrm{Th}} \tag{48}$$

$$0\le\delta_{m,i,1}^{\mathrm{Th}}\le S_{m,i,1}^{\mathrm{Th}}-P_{m,i}^{\mathrm{Th,min}} \tag{49}$$

$$0\le\delta_{m,i,N_i^{\mathrm{Th}}}^{\mathrm{Th}}\le P_{m,i}^{\mathrm{Th,max}}-S_{m,i,N_i^{\mathrm{Th}}-1}^{\mathrm{Th}} \tag{50}$$

$$0\le\delta_{m,i,\tau}^{\mathrm{Th}}\le S_{m,i,\tau}^{\mathrm{Th}}-S_{m,i,\tau-1}^{\mathrm{Th}}\quad\forall\tau\in\left\{2,3,\ldots,N_i^{\mathrm{Th}}\right\} \tag{51}$$

where $FC_{m,i}^{\mathrm{Th},0}$ is the fuel cost of the i^{th} thermal unit located at the m^{th} regional AC grid as it outputs the minimum power; $S_{m,i,\tau}^{\mathrm{Th}}$ denotes the τ^{th} vertex of linear line segments for fuel cost of the i^{th} generator at the m^{th} regional AC grid; $\delta_{m,i,1}^{\mathrm{Th}}$ and $k_{m,i,\tau}^{\mathrm{Th}}$ are the corresponding increment and slope of the τ^{th} linear line segment of the i^{th} generator fuel cost at the m^{th} regional AC grid, respectively; and N_i^{Th} is the total number of linear line segments of the i^{th} generator fuel cost at the m^{th} regional AC grid.

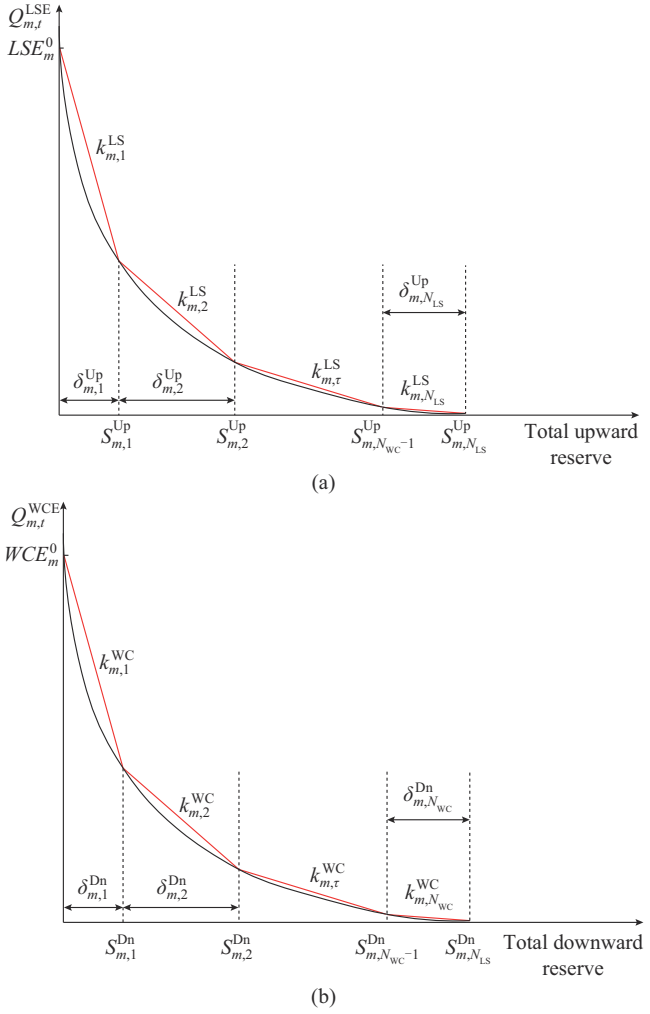

Fig. 3. Piecewise linearization of LSE $Q_{m,t}^{\mathrm{LSE}}$ and WCE $Q_{m,t}^{\mathrm{WCE}}$. (a) $Q_{m,t}^{\mathrm{LSE}}$. (b) $Q_{m,t}^{\mathrm{WCE}}$.

The combination of (2), (4)-(33), and (37)-(51) comprises the proposed FDCCUC model for multiple regional AC grids interconnected by DC tie-lines. Although the formed optimization is an MILP problem, direct computation in a centralized manner conflicts with the fact that global information cannot be fully accessed for the centralized dispatching because regional AC grids are independently managed by different system operators. Therefore, the next section proposes a hierarchical searching algorithm to deal with this issue.

III. Hierarchical Searching Algorithm for FDCCUC Model to Protect Private Scheduling Information of Regional AC Grids

A. Mathematical Principles of Searching Algorithm

The proposed FDCCUC problem can be arranged in the following specific MILP form:

$$\min\sum_{m\in\boldsymbol{A}}\boldsymbol{c}_m^{\mathrm{Obj}}\boldsymbol{x}_m^{\mathrm{Ex}} \tag{52}$$

s.t.

$$\sum_{m\in A}\boldsymbol{B}_m^{\mathrm{Ex,Eq}}\boldsymbol{x}_m^{\mathrm{Ex}}=\boldsymbol{b}^{\mathrm{Ex,Eq}} \tag{53}$$

$$\boldsymbol{EB}_m^{\mathrm{Ex}}\boldsymbol{x}_m^{\mathrm{Ex}}+\boldsymbol{EB}_m^{\mathrm{Int}}\boldsymbol{x}_m^{\mathrm{Int}}=\boldsymbol{b}_m^{\mathrm{Cp,Eq}}\quad\forall m\in A \tag{54}$$

$$\boldsymbol{IB}_m^{\mathrm{Ex}}\boldsymbol{x}_m^{\mathrm{Ex}}+\boldsymbol{IB}_m^{\mathrm{Int}}\boldsymbol{x}_m^{\mathrm{Int}}\le\boldsymbol{b}_m^{\mathrm{Cp,Ineq}}\quad\forall m\in A \tag{55}$$

$$\begin{cases}\boldsymbol{x}_m^{\mathrm{Int}}\ge\boldsymbol{0}\\ \boldsymbol{x}_m^{\mathrm{Ex}}\ge\boldsymbol{0}\end{cases}\quad\forall m\in A \tag{56}$$

$$x_{m,ii}^{\mathrm{Int}}\in\{0,1\}\quad\forall ii\in\Omega_m^{0/1},\forall m\in A \tag{57}$$

where $\boldsymbol{x}_m^{\mathrm{Int}}$ is the vector of decision variables whose information should be hidden internally within the m^{th} regional AC grid, such as $P_{m,i,t}^{\mathrm{Th}}$, $R_{m,i,t}^{\mathrm{Up}}$, $R_{m,i,t}^{\mathrm{Dn}}$, $u_{m,i,t}$, $v_{m,i,t}$, and $z_{m,i,t}$; $x_{m,ii}^{\mathrm{Int}}$ is the ii^{th} binary (0/1) decision variable among $\boldsymbol{x}_m^{\mathrm{Int}}$, i.e., $u_{m,i,t}$, $v_{m,i,t}$, and $z_{m,i,t}$; $\Omega_m^{0/1}$ is the index set of all integer decision variables of the m^{th} regional AC grid; $\boldsymbol{x}_m^{\mathrm{Ex}}$ is the vector of continuous decision variables by which the m^{th} regional AC grid communicates information with other grids, i.e., C_m^{Total}, $P_{m,r,t}^{\mathrm{TLine}}$, $TR_{m,r,t}^{\mathrm{Up}}$, and $TR_{m,r,t}^{\mathrm{Dn}}$; and $\boldsymbol{c}_m^{\mathrm{Obj}}$, $\boldsymbol{B}_m^{\mathrm{Ex,Eq}}$, $\boldsymbol{EB}_m^{\mathrm{Ex}}$, $\boldsymbol{EB}_m^{\mathrm{Int}}$, $\boldsymbol{IB}_m^{\mathrm{Ex}}$, $\boldsymbol{IB}_m^{\mathrm{Int}}$, $\boldsymbol{b}^{\mathrm{Ex,Eq}}$, $\boldsymbol{b}_m^{\mathrm{Cp,Eq}}$, and $\boldsymbol{b}_m^{\mathrm{Cp,Ineq}}$ are the coefficient matrices with proper dimensions. Therefore, (53) is the compact form of (7)-(9); (54) corresponds to (4)-(6), (18)-(20), (25), (39), (40), (43), (44), (47), and (48); and all of the inequality constraints of the FDCCUC problem are then written in the compact forms (55)-(57).

Due to the binary variables, the conventional branch-and-bound (BB) method is employed to solve the MILP problem (52)-(57) [20]. In particular, the branching process of the BB method is schematically depicted in Fig. 4(a). Each branch in this figure carries a triplet (*m*, *ii*, *state*), i.e., the ii^{th} binary variable of the m^{th} regional AC grid has the value of *state* (0 or 1). Thus, the branching path from the root node to the l^{th} node can be recorded by the following triplet set:

$$\Omega_l^{\mathrm{path}}=\left\{(m,ii,state)\middle|\text{root node}\to l^{\mathrm{th}}\text{ node}\right\} \tag{58}$$

By fixing the binary variables along the path according to (58) and relaxing all other binary variables to be continuous within the range [0, 1], a linear programing (LP) problem associated with the l^{th} node can be constructed as:

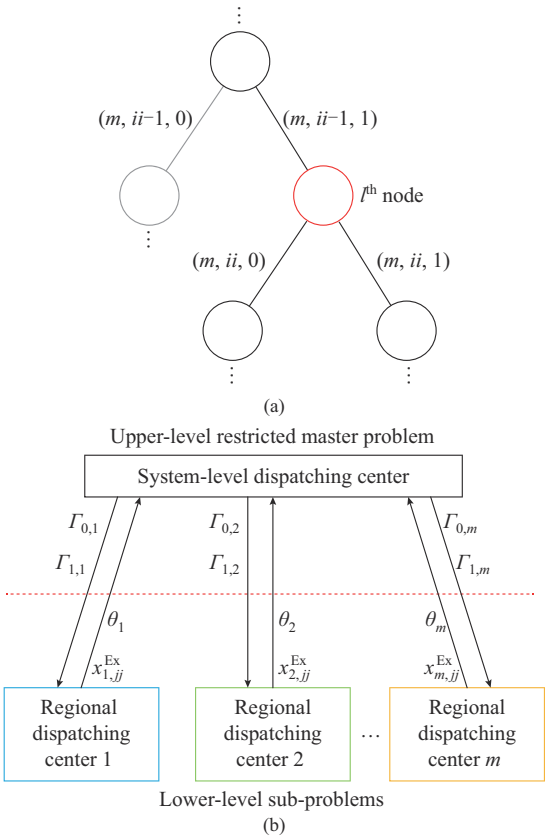

Fig. 4. Illustration of proposed hierarchical searching algorithm. (a) Branching process. (b) Hierarchical distributed iteration process.

$$\begin{cases} O_l = \min \sum_{m\in A} \boldsymbol{c}_m^{\mathrm{Obj}} \boldsymbol{x}_m^{\mathrm{Ex}} \\ \text{s.t.} \sum_{m\in A} \boldsymbol{B}_m^{\mathrm{Ex,Eq}} \boldsymbol{x}_m^{\mathrm{Ex}} = \boldsymbol{b}^{\mathrm{Ex,Eq}} \quad \forall m \in A \\ \boldsymbol{EB}_m^{\mathrm{Ex}} \boldsymbol{x}_m^{\mathrm{Ex}} + \boldsymbol{EB}_{m,l}^{\mathrm{Int}} \boldsymbol{x}_{m,l}^{\mathrm{Int}} = \boldsymbol{b}_{m,l}^{\mathrm{Cp,Eq}} \quad \forall m \in A \\ \boldsymbol{IB}_m^{\mathrm{Ex}} \boldsymbol{x}_m^{\mathrm{Ex}} + \boldsymbol{IB}_{m,l}^{\mathrm{Int}} \boldsymbol{x}_{m,l}^{\mathrm{Int}} \le \boldsymbol{b}_{m,l}^{\mathrm{Cp,Ineq}} \quad \forall m \in A \\ \boldsymbol{x}_{m,l}^{\mathrm{Int}} \ge \boldsymbol{0} \quad \forall m \in A \\ \boldsymbol{x}_m^{\mathrm{Ex}} \ge \boldsymbol{0} \quad \forall m \in A \end{cases} \tag{59}$$

where $\boldsymbol{x}_{m,l}^{\mathrm{Int}}$ is the vector of continuous variables after fixing and relaxing binary variables for the l^{th} node; and O_l is the minimized objective value of the l^{th} node, which also indicates the lower bound of the objective values of child nodes originating from the l^{th} node; and $\boldsymbol{EB}_{m,l}^{\mathrm{Int}}$, $\boldsymbol{IB}_{m,l}^{\mathrm{Int}}$, $\boldsymbol{b}_{m,l}^{\mathrm{Cp,Eq}}$, and $\boldsymbol{b}_{m,l}^{\mathrm{Cp,Ineq}}$ are the coefficient matrices with proper dimensions of the l^{th} node.

In this paper, Dantzig-Wolfe (DW) decomposition is employed to compute the large-scale LP problem (59) [20]. Specifically, the 2nd to 5th constraints in (59) form a polyhedron with a number of extreme points (it is assumed here that the polyhedron is bounded), and any point inside the polyhedron can be expressed in terms of weighted extreme points as:

$$\begin{bmatrix} \boldsymbol{x}_m^{\mathrm{Ex}} \\ \boldsymbol{x}_{m,l}^{\mathrm{Int}} \end{bmatrix} = \sum_{j\in\Omega_{m,l}^{\mathrm{p}}} \eta_{m,l,j} \begin{bmatrix} \bar{\boldsymbol{x}}_{m,j}^{\mathrm{Ex}} \\ \bar{\boldsymbol{x}}_{m,l,j}^{\mathrm{Int}} \end{bmatrix} \tag{60}$$

$$\sum_{j\in\Omega_{m,l}^{\mathrm{p}}} \eta_{m,l,j} = 1 \tag{61}$$

$$\eta_{m,l,j} \ge 0 \quad \forall j \in \Omega_{m,l}^{\mathrm{p}} \tag{62}$$

where $\left[\bar{\boldsymbol{x}}_{m,j}^{\mathrm{Ex}}, \bar{\boldsymbol{x}}_{m,l,j}^{\mathrm{Int}}\right]^{\mathrm{T}}$ is the j^{th} extreme point of the polyhedron of the l^{th} node for the m^{th} regional AC grid; $\eta_{m,l,j}$ is the weight for the j^{th} extreme point of the l^{th} node for the m^{th} regional AC grid; and $\Omega_{m,l}^{\mathrm{p}}$ is the index set of all extreme points of the l^{th} node for the m^{th} regional AC grid. Therefore, according to DW decomposition, searching for the optimal solution of the LP problem (59) consists of iterative computations of the following optimizations.

Step 1: a restricted master problem (RMP) is first formed by using partially known extreme points, as follows:

$$\bar{O}_l = \min \sum_{m\in A} \sum_{j\in\Omega_{m,l}^{\mathrm{rp}}} \eta_{m,l,j} \left(\boldsymbol{c}_m^{\mathrm{Obj}} \bar{\boldsymbol{x}}_{m,l,j}^{\mathrm{Ex}} \right) \tag{63}$$

s.t.

$$\sum_{m\in A} \sum_{j\in\Omega_{m,l}^{\mathrm{rp}}} \eta_{m,l,j} \left(\boldsymbol{B}_m^{\mathrm{Ex,Eq}} \bar{\boldsymbol{x}}_{m,l,j}^{\mathrm{Ex}} \right) = \boldsymbol{b}^{\mathrm{Ex,Eq}} \tag{64}$$

$$\sum_{j\in\Omega_{m,l}^{\mathrm{rp}}} \eta_{m,l,j} = 1 \tag{65}$$

$$\eta_{m,l,j} \ge 0 \quad \forall j \in \Omega_{m,l}^{\mathrm{rp}} \tag{66}$$

where $\bar{O}_l$ is the minimized objective value of the RMP; and $\Omega_{m,l}^{\mathrm{rp}}$ is the subset of $\Omega_{m,l}^{\mathrm{p}}$. The decision variables of the RMP are the weights $\eta_{m,l,j}$. In particular, the RMP is solved with the conventional simplex method to derive the optimal basis multipliers $\boldsymbol{\Gamma}_0$ and $\boldsymbol{\Gamma}_1$, which are two row vectors with proper dimensions.

Step 2: a sub-problem is then constructed based on $\boldsymbol{\Gamma}_0$ for each area m as:

$$\theta_m = \min \left(\boldsymbol{c}_m^{\mathrm{obj}} - \boldsymbol{\Gamma}_0 \boldsymbol{B}_m^{\mathrm{Ex,Eq}} \right) \boldsymbol{x}_m^{\mathrm{Ex}} \tag{67}$$

s.t.

$$\boldsymbol{EB}_m^{\mathrm{Ex}} \boldsymbol{x}_m^{\mathrm{Ex}} + \boldsymbol{EB}_{m,l}^{\mathrm{Int}} \boldsymbol{x}_{m,l}^{\mathrm{Int}} = \boldsymbol{b}_{m,l}^{\mathrm{Cp,Eq}} \tag{68}$$

$$\boldsymbol{IB}_m^{\mathrm{Ex}} \boldsymbol{x}_m^{\mathrm{Ex}} + \boldsymbol{IB}_{m,l}^{\mathrm{Int}} \boldsymbol{x}_{m,l}^{\mathrm{Int}} \le \boldsymbol{b}_{m,l}^{\mathrm{Cp,Ineq}} \tag{69}$$

$$\begin{cases} \boldsymbol{x}_{m,l}^{\mathrm{Int}} \ge \boldsymbol{0} \\ \boldsymbol{x}_m^{\mathrm{Ex}} \ge \boldsymbol{0} \end{cases} \tag{70}$$

where θ_m is the minimized objective value of the sub-problem. Vectors $\boldsymbol{x}_m^{\mathrm{Ex}}$ and $\boldsymbol{x}_{m,l}^{\mathrm{Int}}$ contain the decision variables of this optimization, and the optimal solution based on the simplex method can be represented by $\left[\bar{\boldsymbol{x}}_{m,jj}^{\mathrm{Ex}}, \bar{\boldsymbol{x}}_{m,l,jj}^{\mathrm{Int}}\right]^{\mathrm{T}}$. This solution is actually an extreme point of the polyhedron described by (60) and (61).

Step 3: after solving the above RMP and sub-problems, the following test numbers are computed:

$$\sigma_m = \theta_m - \Gamma_{1,m} \quad \forall m \in A \tag{71}$$

where $\Gamma_{1,m}$ is the m^{th} element of $\boldsymbol{\Gamma}_1$.

Thus, if $\sigma_m \ge 0$ ($\forall m \in A$), the optimal solution of the original LP problem (59) is found and $O_l = \bar{O}_l$; otherwise, the newly obtained extreme points $\bar{\boldsymbol{x}}_{m,jj}^{\mathrm{Ex}}$ ($\forall m \in A$) are added to the RMP ($\Omega_{m,l}^{\mathrm{rp}} = jj \bigcup \Omega_{m,l}^{\mathrm{rp}}$) and *Steps 1* to *3* are repeated.

Once $\bar{O}_l$ is derived, it will be compared with the global lower bound O^{global}: if $O_l > O^{\mathrm{global}}$, the branching process from the l^{th} node will be stopped; else if all slacked decision variables of the LP problem (59) are just binaries, the global

lower bound is replaced by $O^{\text{global}}=O_l$ and all nodes (and their downstream branches) that have the minimized objective values larger than O_l are cut; else, the branching process from the l^{th} node is continued until the end of the searching tree or no feasible solution can be found. Hence, after completing the BB process, the optimal solution of the original MILP problem (52)-(57) can be acquired from the node (the LP problem (59)) that results in the global lower bound O^{global}.

B. Implementation of Searching Algorithm in Hierarchical Manner

This paper proposes that the searching algorithm employed for the FDCCUC problem is implemented in an efficient hierarchical manner, as shown in Fig. 4(b). The upper level is a system-level dispatching center while the lower level consists of all regional dispatching centers. System-level operator only knows the boundary variables and has no knowledge of operational information such as the output of units, load demand and reserve allocation of regional AC grids. More importantly, no information is exchanged between regional grids. Therefore, the proposed decomposition method and searching algorithm show merit in privacy protection. The system-level dispatching center mainly performs the following tasks.

1) Build and maintain the BB searching tree, and master the searching progress.

2) According to the path set Ω_l^{path} of the l^{th} node, pass on the triplet (*m*, *ii*, *state*) to dispatching center *m* to determine how the binary variables belonging to these regional grids are fixed and slacked.

3) Receive θ_m and $\bar{\boldsymbol{x}}_{m,jj}^{\text{Ex}}$ from the regional dispatching centers, compute the RMP, and pass on the derived $\boldsymbol{\Gamma}_0$ and $\boldsymbol{\Gamma}_1$ to all regional dispatching centers.

4) Identify convergence of the searching process for the LP problem (59) associated with the l^{th} node.

The manipulations performed by the regional dispatching centers include:

1) Inform the system-level dispatching center how many binary variables they have and determine fixed and slacked binary variables according to the received triplet (*m*, *ii*, *state*).

2) Compute the sub-problems and pass on the derived θ_m and $\bar{\boldsymbol{x}}_{m,jj}^{\text{Ex}}$ to the system-level dispatching center.

IV. Numerical Simulations

This section validates the proposed FDCCUC model, which is hierarchically solved through numerical simulations. First, the effectiveness of the FDCCUC model in harnessing the reserve capacities of loads based on the LFD effects is demonstrated and compared with the existing models in terms of wind power accommodation capability. Then, the computational efficiency of the hierarchical searching algorithm is tested.

All simulations are performed within the environment of MATLAB 2020a running on a PC with an Intel Core(TM) i7-8700 CPU (3.2 GHz) and 32 GB of memory. Gurobi 9.1.1 is employed for solving LP problems.

A. Test Systems

Two systems, i.e., the 2-area 6-bus system and the 3-area 354-bus system, are used as the testbeds. Figure 5 shows the topology of the 2-area 6-bus system, which has five traditional thermal units (G1-G5) and one wind farm integrated at Bus 2. The parameters and operational constraints of the thermal units are the same as [18] and the installed capacity of the wind farm is 100 MW. The prediction values of wind power and load for a typical summer day (96 dispatching periods) are provided in Fig. 6. The rated capacity of the DC tie-line between the two areas is 100 MW, and the allowable power change ratio is 50 MW per 15 min.

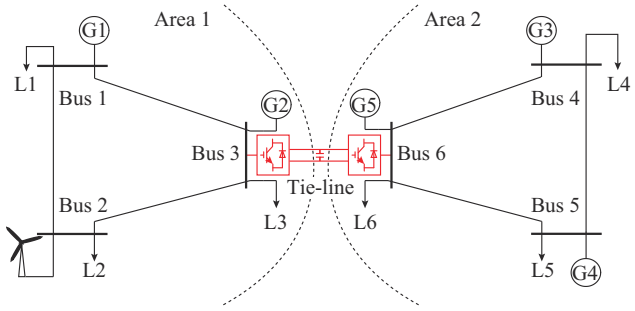

Fig. 5. Topology of 2-area 6-bus system.

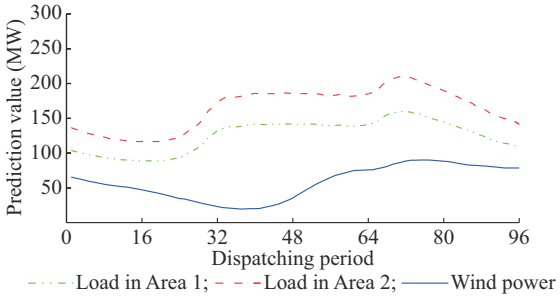

Fig. 6. Prediction values of wind power and load in 2-area 6-bus system for a typical summer day.

The 3-area 354-bus system is composed of three modified IEEE 118-bus systems; the two with wind power integrated are regarded as sending-end systems (SESs), and the remaining one is regarded as a receiving-end system (RES). The aggregated capacities of wind power are 2500 MW at SES#1 and 3000 MW at SES#2. There are two DC tie-lines interconnecting these three regional AC grids: HVDC#1 connects SES#1 and the RES, while HVDC#2 connects SES#2 and the RES.

In addition, according to data records from EirGird, Ireland, the LS cost and wind curtailment penalty (WCP) are set to be 3500 $/MWh and 80 $/MWh, respectively. The upward and downward reserve prices of thermal units used in this paper are 30 $/MWh and 15 $/MWh, respectively [18]. Historical wind power forecasting error data from EirGrid for 2018 to 2020 are used to fit the versatile probability distribution model of the wind power forecasting error. Confidence levels $\bar{c}_m$ and $\underline{c}_m$ are selected to be 95% and 90%, respectively. In the 2-area 6-bus system, the load power sensitivity with respect to frequency is uniformly set to be 2.5% for loads in Area 1 and 1% for loads in Area 2, respectively.

Moreover, the regional AC grids SES#1 and SES#2 of the 3-area 354-bus system have the same load power sensitivity of 2.5% and the RES has a load power sensitivity of 1.5%. The frequency deviation limits are set to be 0.5 Hz for wind-integrated regional grids and 0.2 Hz for load centers which are within the Chinese standard [21].

B. Effectiveness of FDCCUC Model

To verify the effectiveness of the proposed FDCCUC model, economical indices including the thermal unit OC, RC, load shedding penalty (LSP), and WCP are introduced for the 2-area 6-bus system according to (2)-(5). The FDCCUC model will be compared with two other scheduling models commonly found in references in terms of these indices [15], [16]:

1) Model 1: DC tie-line power is adjustable within a permitted range, but no reserve is shared between regional AC grids.

2) Model 2: both power and reserve can be transmitted by DC tie-lines among multiple regional AC grids.

3) Model 3: the proposed FDCCUC model, which considers not only sharing of power and reserve among multiple AC grids, but also extra reserve capacities due to the LFD effects.

The comparison of economical indices for three models in the 2-area 6-bus system are listed in Table I. The total cost of Model 2 is slightly less than that of Model 1 due to less TC. That is generally accepted because Model 2 cannot change the total amounts of reserve demands and reserve resources even though it can coordinate power and reserve among regional AC grids. Once the thermal units have sufficient reserve capacities, the relevant indices RC, LSP, and WCP will be the same. The reserve shared between regional AC grids optimizes the operation sequences of thermal units and reduces the startup/shutdown actions so that the TC drops. In contrast, Model 3 develops additional reserve resources via the permission of safe steady-state frequency deviations and the LFD effects. Therefore, it is not surprising to see overwhelmingly reduced cost indices with Model 3, especially those relevant to reserves such as RC, LSP, and WCP.

TABLE I
COMPARISON OF ECONOMICAL INDICES FOR THREE MODELS IN 2-AREA 6-BUS SYSTEM

Model	TC ($)	RC ($)	LSP ($)	WCP ($)	Total ($)
1	438000	38400	3160	1050	480000
2	429000	38400	3160	1050	472000
3	425000	18300	2850	690	447000

Sensitivity analysis of the penalty coefficient π, which is used to confine the frequency deviation, is conducted. As shown in Fig. 7, when π increases from zero to around 40 $/MW, the total amount of downward reserves carried by thermal units has an increasing trend; the opposite trend is observed for upward reserves. This is because that the proposed FDCCUC model has a general ability to lower the operational frequency so that actually committed loads will shrink and less thermal unit power as well as relevant costs will be required. A larger penalty coefficient π can naturally hinder this ability and force thermal units to generate more power. Accordingly, the upward reserves are reduced while the downward reserves increase. In addition, these two types of reserves remain unchanged for π values larger than 40 $/MW.

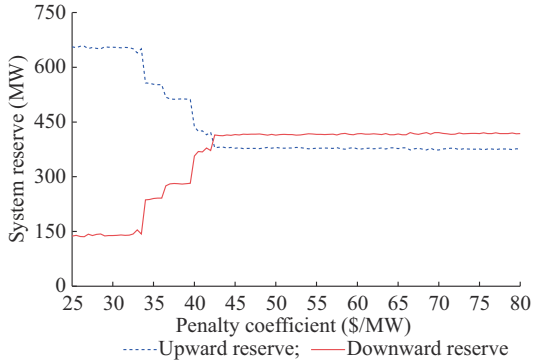

Fig. 7. Sensitivity analysis results of penalizing coefficient π.

Another role of penalty coefficient π is to avoid a large operational frequency deviation which is introduced as a decision variable in this paper to serve as auxiliary reserve source. The maximum permitted frequency deviation for Areas 1 and 2 are set to be 0.5 Hz and 0.2 Hz, respectively [21]. A comparison of operational frequency with different penalty coefficients is demonstrated in Fig. 8, where $\pi_0 = 0$ $/MW and $\pi_1 = 40$ $/MW. As shown in Fig. 8, system operators always intend to operate at permitted frequency limit during the absence of penalty coefficient π.

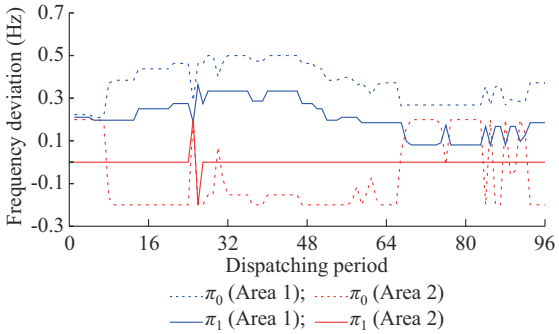

Fig. 8. Simulation results of operational frequency with different penalty coefficients.

As mentioned in the sensitivity analysis, system safety compromises the economy. However, by setting the penalty coefficient to be π_1, the investigating system operates at a minor deviation from nominal values, which maintains a safety margin to frequency limitation (the maximum deviation within one day is less 0.3 Hz for Area 1 and frequency excursion events become less frequent). Note that this frequency limitation is stipulated by Chinese grid operational code for normal condition and smaller than the threshold value of emergency measurement like under frequency load shedding (UFLD). Though the hard constraints (19) - (21) could restrict operational frequency deviation, the frequency deviation penalty could reduce the duration of frequency ex-

cursion. The constant value of π may be not suitable when the load side participates in auxiliary service market. Therefore, a more theoretical method of determination of π should be taken into consideration in the future work.

Figure 9 shows the scheduled power and reserve transmitted through DC tie-line for Models 1 and 3. Clearly, the DC tie-line power is not changeable after scheduling due to security constraints considered in Model 1. In comparison, the reserve ranges scheduled by Model 3 for the DC tie-line (represented by the grey area in Fig. 9) fully consider these security constraints so that Model 3 can operate safely and handle uncertain WPG. Generally, leaving the confidence levels $\bar{c}_m$ and $\underline{c}_m$ unchanged and gradually increasing the capacity of the wind farm will require more reserves to cover increasingly uncertain wind power forecasting error; otherwise, the unexpected wind power will be curtailed. Thus, exploiting the operational flexibilities of DC tie-lines not only reduces the system OCs but also increases the integration levels of wind power, as shown in Fig. 10.

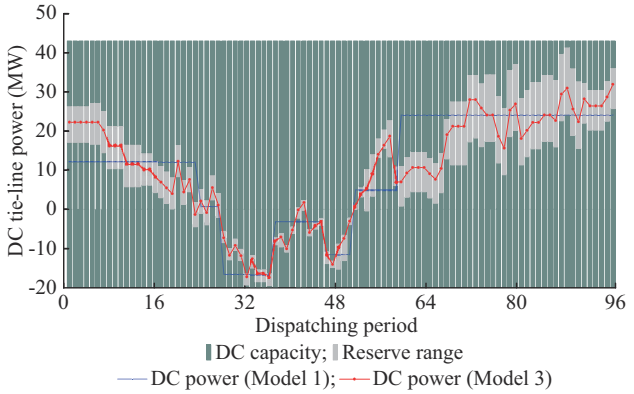

Fig. 9. Scheduled power and reserve transmitted through DC tie-line for Models 1 and 3.

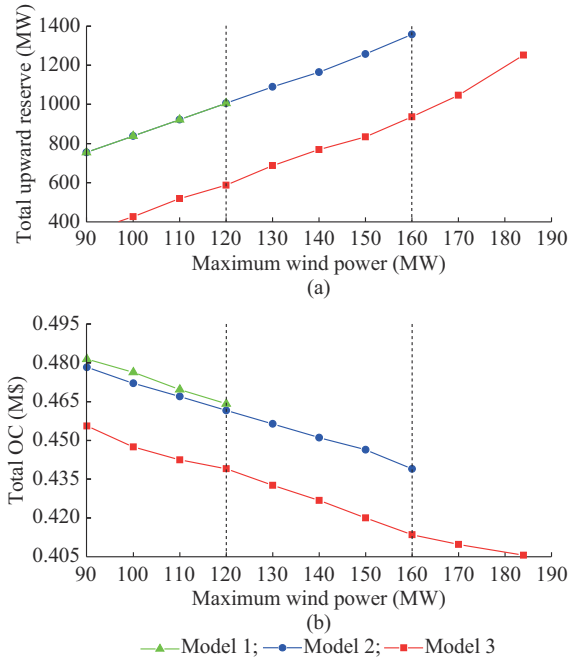

Fig. 10. Simulation results of different models with increasing penetration levels of wind power. (a) Total upward reserve. (b) Total OC.

Provided the same amounts of wind power curtailment result, the maximum wind power is increased from 120 MW in Model 1 to 160 MW in Model 2, and finally to 182 MW in Model 3. In other words, the proposed FDCCUC model can integrate approximately 51% more wind power than the other two models. Although the required reserves increase in each model as the penetration level of wind power increases, the total OC still drops because more free wind energy is utilized by Model 3.

C. Computational Performance of Hierarchically Implemented Searching Algorithm for FDCCUC Model

1) Quality of Optimal Solution

In this subsection, Models 2 and 3 will be further employed to demonstrate the quality of the optimal solution derived by the proposed hierarchical searching algorithm. First, the optimization problems of both scheduling models are solved in a centralized manner using the Gurobi package. The solutions obtained are then used as benchmarks for comparisons with the solutions derived by the hierarchical searching algorithm. Based on the 3-area 354-bus system, comparisons of the economical indices are detailed in Table II.

Table II clearly shows that, for both Models 2 and 3, the hierarchical searching algorithm finds the optimal solutions that have few differences from their benchmarks. This means the DW decomposition-based hierarchical searching algorithm can guarantee the quality of the solutions found. In addition, the comparison of the RC, LSP, and WCP indices between Models 2 and 3 shows that slacking operational frequency to release potential reserves based on the LFD effects together with scheduling DC tie-lines to carry reserves can significantly reduce various system OCs, especially those tightly relevant to system reserves.

TABLE II
COMPARISON OF ECONOMICAL INDICES FOR 3-AREA 354-BUS SYSTEM

Model	Algorithm	TC ($)	RC ($)	LSP ($)	WCP ($)	Total ($)
2	Centralized	2217900	489630	39552	17204	2764300
	Hierarchical	2217800	489610	39550	17203	2764200
3	Centralized	2184700	223300	35672	11305	2458300
	Hierarchical	2184600	223290	35671	11305	2458200

2) Time Consumption of Searching Process

In the 3-area 354-bus system, three regional AC grids are deployed with three regional dispatching centers that carry out computations of sub-problems and communicate with a system-level dispatching center that computes the RMP. Specifically, one computational iteration is defined as solving the RMP and then each of the three individual sub-problems (bearing in mind that several such iterations may be required to accomplish computations of each node during the BB process). Moreover, because the sub-problems can be solved by the regional dispatching centers in parallel, the time consumption of an iteration is defined as $T^{\mathrm{RMP}}+\max\{T_m^{\mathrm{SP}}, m\in A\}$, where T^{RMP} is the solution time of the RMP and T_m^{SP} is the solution time of the m^{th} sub-problem. In addition, the MILP problem formulated by the proposed FDCCUC model for the 3-area 354-bus system has 60094 decision variables

among which 11664 variables are binaries. Finally, the proposed hierarchical searching algorithm takes 9418 iterations to converge. The time consumptions of these iterations are also statistically analyzed and the CDF of the time consumption of each iteration is plotted in Fig. 11. About 90% of the iterations require less than 1 s.

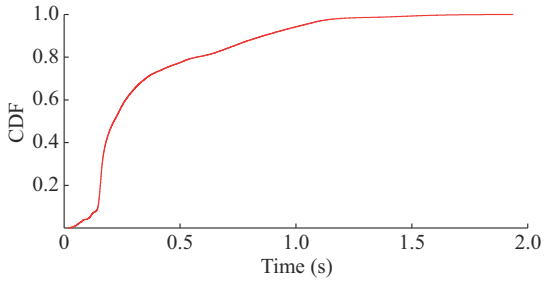

Fig. 11. CDF of computation time of each iteration.

The total time cost of the hierarchical searching algorithm in terms of the sum of the time consumed by all iterations is about 97 min. Notably, the current version of the hierarchical searching algorithm is somewhat inefficient compared with the commercial package Gurobi, which can directly solve the formulated MILP problem in around 5 min. This huge gap in computational efficiency is primarily due to the BB method used by the hierarchical searching algorithm, which is still far from optimal; future studies could considerably improve the searching efficiency of the proposed hierarchical searching algorithm. Even so, the current version of the hierarchical searching algorithm is obviously suitable for day-ahead scheduling and, most importantly, it keeps regional information hidden during the searching process.

V. Conclusion

Mining operational flexibilities of loads is a hot trend for power systems to confront the problems caused by the increasing integration of WPG. Thus, by introducing an auxiliary reserve released from LFD effect, this paper proposes an FDCCUC model together with a customized hierarchical searching algorithm to promote the ability of bulk AC/DC hybrid power systems to accommodate uncertain wind power. Optimization model derivations and numerical simulations lead to the following conclusions: ① the proposed reserve is practically feasible and low-cost, and can be released by changing the system operational frequency within a permitted safe range; ② the additional reserve based on the LFD effect is effective when reducing the WCE and LSE, i.e., it allows systems to endure more uncertain wind power forecasting error and permits the installation of larger wind power capacities; ③ the necessity of scheduling reserves transmitted by DC tie-lines in the FDCCUC model is demonstrated, otherwise the cross-regional reserve share may be unexpectedly restricted by technical constraints of the DC tie-lines; and ④ in contrast with centralized algorithm, the proposed hierarchical searching algorithm derives almost the same high-quality solutions but requires quite limited information exchange between distributed dispatching centers. Although this exploratory research facilitates renewable penetration levels without expansion of traditional reserve resources, future work should focus on theoretical methods to restrict frequency deviation.

References

[1] R. Doherty and M. O'Malley, "A new approach to quantify reserve demand in systems with significant installed wind capacity," *IEEE Transactions on Power Systems*, vol. 20, no. 2, pp. 587-595, May 2005.

[2] Y. Yang, C. Qin, Y. Zeng *et al*., "Optimal coordinated bidding strategy of wind and solar system with energy storage in day-ahead market," *Journal of Modern Power Systems and Clean Energy*, vol. 10, no. 1, pp. 192-203, Jan. 2022.

[3] J. Suh, D. Yoon, Y. Cho *et al*., "Flexible frequency operation strategy of power system with high renewable penetration," *IEEE Transactions on Sustainable Energy*, vol. 8, no. 1, pp. 192-199, Jan. 2017.

[4] L. Badesa, F. Teng, and G. Strbac, "Simultaneous scheduling of multiple frequency services in stochastic unit commitment," *IEEE Transactions on Power Systems*, vol. 34, no. 5, pp. 3858-3868, Sept. 2019.

[5] T. Nguyen, H. Yoo, and H. Kim, "A droop frequency control for maintaining different frequency qualities in a stand-alone multimicrogrid system," *IEEE Transactions on Sustainable Energy*, vol. 9, no. 2, pp. 599-609, Apr. 2018.

[6] S. K. Pradhan and D. K. Das, "H_∞ load frequency control design based on delay discretization approach for interconnected power systems with time delay," *Journal of Modern Power Systems and Clean Energy*, vol. 9, no. 6, pp. 1468-1477, Nov. 2021.

[7] X. Tian, Y. Chi, C. Liu *et al*., "Power-balancing coordinated control of wind power and demand-side response under post-fault condition," *Journal of Modern Power Systems and Clean Energy*, vol. 10, no. 5, pp. 1207-1215, Sept. 2022.

[8] P. Kundur, N. J. Balu, and M. G. Lauby, *Power System Stability and Control*. New York: McGraw-Hill, 1994.

[9] S. Liao, J. Xu, Y. Sun *et al*., "Load-damping characteristic control method in an isolated power system with industrial voltage-sensitive load," *IEEE Transactions on Power Systems*, vol. 31, no. 2, pp. 1118-1128, Mar. 2016.

[10] Y. Zhou, M. Cheng, and J. Wu, "Enhanced frequency response from industrial heating loads for electric power systems," *IEEE Transactions on Industrial Informatics*, vol. 15, no. 6, pp. 3388-3399, Jun. 2019.

[11] C. Wei, J. Xu, S. Liao *et al*., "Aggregation and scheduling models for electric vehicles in distribution networks considering power fluctuations and load rebound," *IEEE Transactions on Sustainable Energy*, vol. 11, no. 4, pp. 2755-2764, Oct. 2020.

[12] C. Wei, J. Xu, S. Liao *et al*., "Coordination optimization of multiple thermostatically controlled load groups in distribution network with renewable energy," *Applied Energy*, vol. 231, pp. 456-467, Dec. 2018.

[13] Y. Bao, J. Xu, W. Feng *et al.*, "Provision of secondary frequency regulation by coordination dispatch of industrial loads and thermal power plants," *Applied Energy*, vol. 242, pp. 302-312, May 2019.

[14] Y. Li, X. Qiao, C. Chen *et al*., "Integrated optimal siting and sizing for VSC-HVDC-link-based offshore wind farms and shunt capacitors," *Journal of Modern Power Systems and Clean Energy*, vol. 9, no. 2, pp. 274-284, Mar. 2021.

[15] R. Martínez-Parrales, C. R. Fuerte-Esquivel, B. A. Alcaide-Moreno *et al*., "A VSC-based model for power flow assessment of multi-terminal VSC-HVDC transmission systems," *Journal of Modern Power Systems and Clean Energy*, vol. 9, no. 6, pp. 1363-1374, Nov. 2021.

[16] X. Zheng, Y. Chen, H. Chen *et al*., "Loss-minimizing generation unit and tie-line scheduling for asynchronous interconnection," *IEEE Journal of Emerging and Selected Topics in Power Electronics*, vol. 6, no. 3, pp. 1095-1103, Sept. 2018.

[17] M. Rayati, A. Sheikhi, A. M. Ranjbar *et al*., "Optimal equilibrium selection of price-maker agents in performance-based regulation market," *Journal of Modern Power Systems and Clean Energy*, vol. 10, no. 1, pp. 204-212, Jan. 2022.

[18] H. Jiang, J. Xu, Y. Sun *et al*., "Dynamic reserve demand estimation model and cost-effectivity oriented reserve allocation strategy for multi-area system integrated with wind power," *IET Generartion, Transmission & Distribution*, vol. 12, no. 7, pp. 1606-1620, Apr. 2018.

[19] G. Morales-España, R. Baldick, J. García-González *et al*., "Power-capacity and ramp-capability reserves for wind integration in power-based UC," *IEEE Transactions on Sustainable Energy*, vol. 7, no. 2, pp. 614-624, Apr. 2016.

[20] C. Wei, Q. Wu, J. Xu *et al*., "Distributed scheduling of smart buildings to smooth power fluctuations considering load rebound," *Applied Energy*, vol. 276, p. 115396, Oct. 2020.
[21] *The Grid Operation Code*, GB/T31464-2015, 2015.

Rui Chen received the B.S. degree in electrical engineering and automation from Hubei University of Technology, Wuhan, China, in 2016, and the M.S. degree in electrical power system engineering from University of Manchester, Manchester, UK, in 2017. He is currently working toward the Ph.D. degree in the School of Electrical Engineering and Automation, Wuhan University, Wuhan, China. His research interests include power system dynamics and control, wind power, and economic operation of power systems.

Deping Ke received the B. S. degree in electrical engineering from Huazhong University of Science and Technology, Wuhan, China, in 2005, and the Ph.D. degree in electrical engineering from The Hong Kong Polytechnic University, Hong Kong, China, in 2012. He is currently an Associate Professor with the School of Electrical Engineering and Automation, Wuhan University, Wuhan, China. His research interests include power system dynamics and control and economic operation of power systems.

Yuanzhang Sun received the B.S. degree from Wuhan University of Hydro and Electrical Engineering, Wuhan, China, in 1987, the M. S. degree from the Electric Power Research Institute (EPRI), Beijing, China, in 1982, and the Ph. D. degree in electrical engineering from Tsinghua University, Beijing, China, in 1988. He is currently a Professor of the School of Electrical Engineering with Wuhan University, Wuhan, China, and a Chair Professor of the Department of Electrical Engineering and Vice Director of the State Key Lab of Power System Control and Simulation, Tsinghua University, Beijing, China. His main research interests include power system dynamics and control, wind power, voltage stability and control, and reliability.

C. Y. Chung received the Ph.D. degree in electrical engineering from The Hong Kong Polytechnic University, Hong Kong, China, in 1999. He is currently a Professor and the SaskPower Chair in power systems engineering with the Department of Electrical and Computer Engineering, University of Saskatchewan, Saskatoon, Canada. He is Member of IEEE PES Fellows Evaluation Committee, Senior Editor of IEEE Transactions on Power Systems, Editor of the IEEE Transactions on Sustainable Energy, Vice Editor-in-Chief of the Journal of Modern Power Systems and Clean Energy, and Subject Editor of IET Generation, Transmission & Distribution. His research interests include power system stability/control, planning and operation, computational intelligence applications, electricity markets, and electric vehicle charging.

Haotian Wu received the B. S. degree in electrical engineering from Wuhan University, Wuhan, China, in 2020. He is currently working toward the Ph.D. degree with the School of Electrical Engineering and Automation, Wuhan University. His research interests include probabilistic forecast and stochastic economic dispatch of power systems.

Siyang Liao received the B. S. and Ph. D. degrees in electrical engineering from Wuhan University, Wuhan, China, in 2011 and 2016, respectively. He is currently an Associate Professor with the School of Electrical Engineering and Automation, Wuhan University. His research interests include wind power integration and power system simulation.

Jian Xu received the B.S. and Ph.D. degrees in electrical engineering from Wuhan University, Wuhan, China, in 2002 and 2007, respectively. He is currently a Professor with the School of Electrical Engineering and Automation, Wuhan University. During 2013-2014, he was a Visiting Scholar with the Energy Systems Innovation Center, Washington State University, Pullman, USA. His research interests include power system operation, voltage stability, and wind power control and integration.

Congying Wei received the B.S. and Ph.D. degrees in electrical engineering from Wuhan University, Wuhan, China, in 2016 and 2021, respectively. He is currently working as grid Dispatcher for Central China Branch of State Grid Corporation of China, Wuhan, China. His research interests include distributed load management and power system operation.